Journal of Magnetism and Magnetic Materials 593 (2024) 171846

Contents lists available at ScienceDirect

Journal of Magnetism and Magnetic Materials

journal homepage: www.elsevier.com/locate/jmmm

Research article

Thermodynamic description for magneto-plastic coupling in electrical steel sheets

J. Taurines [a,b,*], F. Martin [a], P. Rasilo [b], A. Belahcen [a]

[a] Department of Electrical Engineering and Automation, Aalto University, Espoo, Finland
[b] Electrical Engineering Unit, Tampere University, Tampere, Finland

ARTICLE INFO

Keywords:
Invariants
Iron-silicon alloys
Magneto-mechanical coupling
Plasticity

ABSTRACT

The purpose of the study is to propose a thermodynamic description of the full magneto-mechanical coupling in electrical steel sheets, including both elasticity and plasticity influence. Kinematic and isotropic hardening are considered as state variables and included to a second-order magneto-elastic energy written as a function of cubic invariants. The simulation of magnetic behaviour of plastified samples subjected to several elastic stresses reproduce the general trends of measurements carried out on non-oriented Fe-3%Si sheets.

1. Introduction

The electrical steel sheets used in the manufacture of rotating electrical machines are affected by numerous mechanical stresses during their life cycle. During manufacture, plastification occurs during the cutting and punching processes. In addition, mechanical stresses in service can reach several MPa for massive rotors. These different mechanical loadings have a great influence on the magnetic behaviour [1].

Indeed, the non-oriented (NO) Fe-3%Si alloy is known to have a so-called second-order behaviour in the magneto-elastic coupling [2], i.e., having an initial susceptibility as a function of mechanical stress passing through a maximum with increasing tensile stress. Moreover, increasing plasticity implies a drop in initial susceptibility [3,4].

Several approaches have been proposed in the literature to describe magneto-elasto-plastic coupling. Shi et al. [5] consider that stress and plastic strain contribute to an effective field. This formulation is uniaxial and the plastic state is only described using the plastic strain. Domenjoud and Daniel [6] consider both the influence of the dislocation rate and the additional stress due to plasticity, maintaining a uniaxial framework. Hubert and Lazreg [7] propose a multiaxial description using only kinematic hardening. In this paper, we propose to extend previous studies which do not provide a multiaxial formulation involving kinematic and isotropic hardenings. Second-order magneto-elastic effects are taken into account by identifying the material constants involved in a recent invariant model [8].

2. Formulation of magneto-elastic coupling

The internal energy density u at any scale is a function of the following extensive thermodynamic variables: the entropy density s, the magnetization $\boldsymbol{m}$ and the total strain $\boldsymbol{\epsilon}$. The internal energy density variation is the sum of the magnetic, mechanical and thermal powers so that

$$\dot{u}(\boldsymbol{m},\boldsymbol{\epsilon},s) = \mu_0 \boldsymbol{h}\cdot\dot{\boldsymbol{m}} + \boldsymbol{\sigma} : \dot{\boldsymbol{\epsilon}} + T\dot{s}. \tag{1}$$

where μ_0 is the permeability of free space, $\boldsymbol{h}$ is the magnetic field, $\boldsymbol{\sigma}$ is the stress tensor and T is the temperature. The use of a Legendre transformation leads to the definition of the Helmoltz free energy density f which is a function not of entropy but of temperature T. A new Legendre transformation is used to define the free enthalpy density Ψ. The Gibbs free energy density [9] is defined using a last Legendre transformation such that

$$g(\boldsymbol{h},\boldsymbol{\sigma},T) = \Psi(\boldsymbol{m},\boldsymbol{\sigma},T) - \mu_0 \boldsymbol{h}\cdot\boldsymbol{m} \tag{2}$$

where $\mu_0\boldsymbol{h}\cdot\boldsymbol{m}$ is the Zeeman energy density. Using (1), the magnetization, the total strain and the entropy respect the equations of state

$$\boldsymbol{m} = -\frac{1}{\mu_0}\frac{\partial g(\boldsymbol{h},\boldsymbol{\sigma},T)}{\partial \boldsymbol{h}} \quad \boldsymbol{\epsilon} = -\frac{\partial g(\boldsymbol{h},\boldsymbol{\sigma},T)}{\partial \boldsymbol{\sigma}} \quad s = -\frac{\partial g(\boldsymbol{h},\boldsymbol{\sigma},T)}{\partial T}. \tag{3}$$

It can be assumed in first approximation that the transformations are isothermal: the free enthalpy and Gibbs free energy densities do not depend on the temperature. Writing Ψ allows to determine the associated variables using (2) and (3). For this purpose, Ψ can be decomposed into three parts so that

$$\Psi(\boldsymbol{m},\boldsymbol{\sigma}) = \Psi^{\mathrm{mec}}(\boldsymbol{\sigma}) + \Psi^{\mathrm{coupl}}(\boldsymbol{m},\boldsymbol{\sigma}) + \Psi^{\mu}(\boldsymbol{m}). \tag{4}$$

* Corresponding author at: Department of Electrical Engineering and Automation, Aalto University, Espoo, Finland.
E-mail address: julien.taurines@aalto.fi (J. Taurines).

https://doi.org/10.1016/j.jmmm.2024.171846
Received 9 October 2023; Received in revised form 9 February 2024; Accepted 10 February 2024
Available online 12 February 2024

The mechanical part Ψ^{mec} (at this point purely elastic) involves the compliance tensor $\mathbf{S}$ [10] such that

$$\Psi^{\text{mec}}(\boldsymbol{\sigma}) = \frac{1}{2}\boldsymbol{\sigma} : \mathbf{S} : \boldsymbol{\sigma}. \tag{5}$$

The purely magnetic part Ψ^{μ} contains the anisotropy energy density and exchange energy density [9] such that

$$\Psi^{\mu}(\boldsymbol{m}) = K_1(\gamma_1^2\gamma_2^2 + \gamma_2^2\gamma_3^2 + \gamma_1^2\gamma_3^2) + K_2(\gamma_1^2\gamma_2^2\gamma_3^2) + A\nabla\boldsymbol{\gamma} : \nabla\boldsymbol{\gamma} \tag{6}$$

where $\boldsymbol{\gamma}$ is the direction of the magnetization, K_1 and K_2 are the magnetocrystalline constants and A is the exchange constant. Regarding the coupling energy Ψ^{coupl} several propositions are available in the literature. We have chosen an invariant formulation at the scale of the magnetic domain recently proposed in the literature, i.e. which verifies

$$\Psi^{\text{coupl}}(\boldsymbol{m}, \boldsymbol{\sigma}) = \Psi^{\text{coupl}}(r \star \boldsymbol{m}, r \star \boldsymbol{\sigma}) \quad \forall r \in \mathbb{O} \tag{7}$$

with $\mathbb{O}$ the full octahedral group. Such a function is proposed in [8] :

$$\begin{aligned}\Psi^{\text{coupl}} = {} & c_{210}\boldsymbol{\sigma}^{\text{d}} : (\boldsymbol{m}\otimes\boldsymbol{m})^{\text{d}} + c_{201}\boldsymbol{\sigma}^{\bar{\text{d}}} : (\boldsymbol{m}\otimes\boldsymbol{m})^{\bar{\text{d}}} + \\ & \frac{c_{220}(\boldsymbol{\sigma}^{\text{d}})^2 : (\boldsymbol{m}\otimes\boldsymbol{m})^{\text{d}} + c^{\text{b}}_{202}(\boldsymbol{\sigma}^{\bar{\text{d}}})^2 : (\boldsymbol{m}\otimes\boldsymbol{m})^{\bar{\text{d}}}}{1 + \delta\sqrt{\frac{3}{2}(\boldsymbol{\sigma}^{\text{d}} + \beta\boldsymbol{\sigma}^{\bar{\text{d}}}) : (\boldsymbol{\sigma}^{\text{d}} + \beta\boldsymbol{\sigma}^{\bar{\text{d}}})}} + \\ & \frac{c^{\text{a}}_{202}(\boldsymbol{\sigma}^{\bar{\text{d}}})^2 : (\boldsymbol{m}\otimes\boldsymbol{m})^{\text{d}} + c_{211}(\boldsymbol{\sigma}^{\bar{\text{d}}}\boldsymbol{\sigma}^{\text{d}}) : (\boldsymbol{m}\otimes\boldsymbol{m})^{\bar{\text{d}}}}{1 + \delta\sqrt{\frac{3}{2}(\boldsymbol{\sigma}^{\text{d}} + \beta\boldsymbol{\sigma}^{\bar{\text{d}}}) : (\boldsymbol{\sigma}^{\text{d}} + \beta\boldsymbol{\sigma}^{\bar{\text{d}}})}}\end{aligned} \tag{8}$$

where $(\bullet)^{\text{d}}$ and $(\bullet)^{\bar{\text{d}}}$ refer to the diagonal and anti-diagonal parts. Denoting $\mathbf{I}$ the fourth order identity tensor, $\mathbf{1}$ the second order identity tensor and $\boldsymbol{e}_i$ the canonical basis of the cube, these projections are defined as

$$(\bullet)^{\text{d}} = \left[\mathbf{I} - \frac{1}{3}\mathbf{1}\otimes\mathbf{1} - \frac{1}{2}\sum_{i<j}\boldsymbol{e}_{ij}\otimes\boldsymbol{e}_{ij}\right] : (\bullet) \tag{9}$$

and

$$(\bullet)^{\bar{\text{d}}} = \frac{1}{2}\sum_{i<j}\boldsymbol{e}_{ij}\otimes\boldsymbol{e}_{ij} : (\bullet) \tag{10}$$

with

$$\boldsymbol{e}_{ij} = \boldsymbol{e}_i\otimes\boldsymbol{e}_j + \boldsymbol{e}_j\otimes\boldsymbol{e}_i \quad (i \neq j). \tag{11}$$

The first material coefficients are directly related to the usual magnetostrictive constants [8] so that

$$c_{210} = -\frac{3}{2M_s^2}\lambda_{100} \quad \text{and} \quad c_{201} = -\frac{3}{2M_s^2}\lambda_{111} \tag{12}$$

with M_s the saturation magnetization. The parameters c_{220}, c^{a}_{202}, c^{b}_{202}, c_{211}, δ and β are so-called second-order material constants. In the absence of more detailed studies on the topic, they have to be identified numerically for each material.

3. Simulations of Fe-3%Si magneto-elastic behaviour

3.1. Simplified multiscale model

For this study, the Gibbs free energy has been expressed at the scale of one magnetic domain (α). For simplification reasons, we have neglected the effects of incompatibilities, i.e. the magnetic field and stress are homogeneous in each grain (gr) and each domain such that

$$\boldsymbol{H} = \boldsymbol{h}_{\text{gr}} = \boldsymbol{h}_{\alpha} \quad \text{and} \quad \boldsymbol{\sigma} = \boldsymbol{\sigma}_{\text{gr}} = \boldsymbol{\sigma}_{\alpha}. \tag{13}$$

It is common practice and more accurate to use an iterative self-consistent scheme [11], but we have preferred to maintain this hypothesis for the purpose of describing the various concepts. The extension to the use of localization consists of considering plastic variables homogeneous at the grain scale, in the same way as elastic variables.

Table 1
Material constants for Fe-3%Si.

Parameter	Value
M_s	$1.61 \cdot 10^{-6}$ A m^{-1}
χ^0	9600
K_1	38 kJ m^{-3}
K_2	0 kJ m^{-3}
λ_{100}	23 ppm
λ_{111}	−4.5 ppm

Table 2
Identified second order magneto-elastic constants.

Parameter	Value
c_{220}	$2.83 \cdot 10^{-18}$ MPa^{-1} A^{-2} m^2
c^{a}_{202}	$1.70 \cdot 10^{-18}$ MPa^{-1} A^{-2} m^2
c^{b}_{202}	$1.41 \cdot 10^{-18}$ MPa^{-1} A^{-2} m^2
c_{211}	0 MPa^{-1} A^{-2} m^2
δ	$4.69 \cdot 10^{-2}$ MPa^{-1}
β	1

Based on (13), the Gibbs free energy g_{α} is written explicitly for any macroscopic loading $(\boldsymbol{H}, \boldsymbol{\sigma})$. The local magnetization is then

$$\boldsymbol{m}_{\alpha} = M_s\boldsymbol{\gamma}_{\alpha} \tag{14}$$

with

$$\boldsymbol{\gamma}_{\alpha} = \arg\min(g_{\alpha}). \tag{15}$$

According to (3) the magnetostriction is

$$\boldsymbol{\epsilon}_{\alpha} = -\frac{\partial g_{\alpha}(\boldsymbol{h}_{\alpha}, \boldsymbol{\sigma}_{\alpha})}{\partial\boldsymbol{\sigma}_{\alpha}}. \tag{16}$$

Based on the work of Chikazumi [12], Buiron et al. [13] have introduced a material parameter A_s that allows the evolution of the volume fraction f_{α} of each domain to be described using a Boltzmann distribution such that

$$f_{\alpha} = \frac{\exp[-A_s g_{\alpha}(\boldsymbol{h}_{\alpha}, \boldsymbol{\sigma}_{\alpha})]}{\sum_{\alpha}\exp[-A_s g_{\alpha}(\boldsymbol{h}_{\alpha}, \boldsymbol{\sigma}_{\alpha})]}. \tag{17}$$

This parameter is directly related to the initial susceptibility χ^0 (see [11]) so that

$$A_s = \frac{3\chi^0}{\mu_0 M_s^2}. \tag{18}$$

Knowing magnetization $\boldsymbol{m}_{\alpha}$, magnetostriction $\boldsymbol{\epsilon}^{\mu}_{\alpha}$ and volume fraction f_{α} for each domain, the grain scale magnetostriction and magnetization are

$$\boldsymbol{\epsilon}^{\mu}_{\text{gr}} = \sum_{\alpha} f_{\alpha}\boldsymbol{\epsilon}^{\mu}_{\alpha} \quad \text{and} \quad \boldsymbol{m}_{\text{gr}} = \sum_{\alpha} f_{\alpha}\boldsymbol{m}_{\alpha}. \tag{19}$$

The macroscopic magnetostriction and magnetization are then obtained by averaging the behaviour of each grain, i.e

$$\boldsymbol{\epsilon}^{\mu} = \sum_{\text{gr}} f_{\text{gr}}\boldsymbol{\epsilon}^{\mu}_{\text{gr}} \quad \text{and} \quad \boldsymbol{M} = \sum_{\text{gr}} f_{\text{gr}}\boldsymbol{m}_{\text{gr}} \tag{20}$$

where f_{gr} is the volume fraction of each grain.

3.2. Simulations results

The material coefficients used are those commonly found in the literature for Fe-3%Si [9] and are given in Table 1. The exchange constant A is taken to be 0 in the absence of an orientation gradient at the domain scale. The six second-order material constants have been numerically identified using least squares error of longitudinal and transverse magnetostrictions between the model and the experimental measurements performed in [14]. The values are given in Table 2.

One can see in Fig. 1 that the model correctly represents the change in monotonicity characteristic of Fe-3%Si, as well as the change in sign of its magnetostriction. Then, the model can be enriched with the magneto-plastic coupling. This is the focus of the next section.

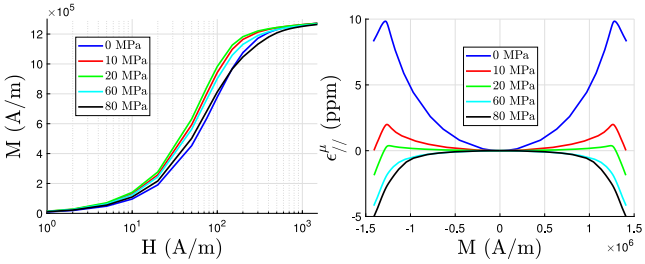

Fig. 1. Simulations of anhysteretic magnetization (left) and anhysteretic magnetostriction (right) for different applied stresses in the elastic domain.

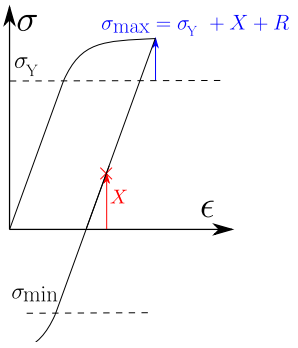

Fig. 2. Evolution of kinematic and isotropic hardening.

4. Including plasticity

Numerous studies have reported on the influence of plasticity on the magnetic behaviour. In particular, they emphasize the influence of dislocation density [3,15]. Considering only this parameter is insufficient because it does not allow to take into account the sign of the plastic deformation. However, the behaviour differs between tension and compression as shown by [16]. Sablik et al. have proposed an approach that takes into account both the amount of dislocation and the hardening [17,18]. This approach, although sufficient for uniaxial plasticity, is simplifying since it reduces plasticity to two scalars which are not consistent with a thermodynamic description. Isotropic plasticity is indeed described by two independent thermodynamic state variables:

- the kinematic hardening $\mathbf{X}$ which is a second-order deviatoric symmetric tensor. It works as a shift of the stress tensor;
- the isotropic hardening R which is a scalar and corresponds to a change of size of the elastic domain.

The experimental identification of these two quantities requires the performance of cycle tests. Indeed, as shown in Fig. 2, tension is not sufficient to decouple the quantities since the stress reached in the plastic domain is written as the sum of the yield stress σ_Y and the two types of hardening. The distinction is only possible after plasticity in compression by measuring the elasticity limits in compression σ_{min} and tension σ_{max}.

However, plastifying thin sheets in compression is tricky due to the high risk of buckling. The contribution of each hardening has been therefore considered as an additional parameter.

4.1. Adding kinematic and isotropic hardenings

As mentioned before, the kinematic hardening $\mathbf{X}$ is a second-order deviatoric symmetric tensor which corresponds to the displacement of the elastic surface. Thus, the magneto-mechanical free enthalpy density is written as

$$\Psi^{coupl}(\boldsymbol{m}, \boldsymbol{\sigma}, \mathbf{X}) = \Psi^{coupl}(\boldsymbol{m}, \boldsymbol{\sigma} - \mathbf{X}). \tag{21}$$

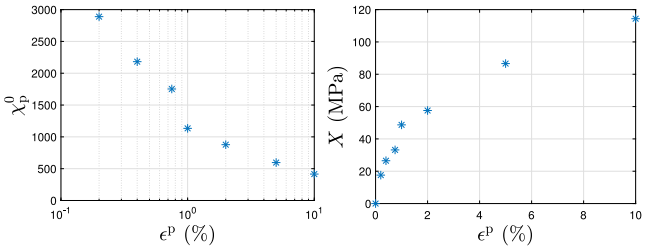

Fig. 3. (χ_p^0, X) estimated for several levels of plasticity.

An immediate consequence of this assumption is that the material constants that are involved in the magneto-elastic formulation (given in Tables 1 and 2) are still valid and new parameters are not needed.

We assume that isotropic hardening does not affect Ψ^{coupl} but influences the initial susceptibility directly. Indeed, several works suggest that the magnetic susceptibility decreases with respect to the square root of the dislocation rate N [3,15]. Moreover, the hardening of the material is proportional to $\sqrt{N}$ [10]. In agreement with these two ideas, Domenjoud et Daniel [6] proposed an evolution of initial susceptibility χ_p^0 (which depends on the level of plasticity) inversely proportional to hardening σ_u such that

$$\chi_p^0 = \frac{\chi^0}{1 + c\sigma_u} \tag{22}$$

with c a material constant. We propose here to keep this form but to modify the expression of σ_u: Domenjoud et al. [6] used two Ludwik laws to express two regimes of evolution of σ_u. This is an approximation that we correct by keeping the exact definition of the strain hardening which is the sum of the isotropic and kinematic hardening. Thus,

$$\sigma_u = R + J_2(\mathbf{X}) \tag{23}$$

with $J_2(\bullet) = \sqrt{\frac{3}{2}\bullet' : \bullet'}$ the second invariant of a second order tensor [10]. The term $\bullet'$ is the deviatoric part of $\bullet$. One can remark that $J_2(\boldsymbol{\sigma})$ is the von Mises stress. In the case of uniaxial tests, $J_2(\mathbf{X}) = X$ as described in Fig. 2.

4.2. Application to Fe-3%Si

Several samples were cut from electrical 0.5 mm thick NO Fe-3%Si electrical steel sheet and plastified in tension at a given plastic strain. They were then magnetically loaded under fixed mechanical stress imposed by a tensile testing machine. The values of χ_p^0 and X were identified using magnetization measurements for each plastic state. A serious drawback is that the two hardenings are not distinguishable with uniaxial tensile tests to identify c. This will be remedied in the future by cyclic testing on one set of samples while another set will be plastified up to the same plasticity level in tension with initial susceptibility measurement. Nevertheless, one can see in Fig. 3 that the order of magnitude of X and its evolution are plausible. One can also note a quasi-exponential decrease of χ_p^0.

Fig. 4 shows both experimental and simulation results for $\epsilon^p = 0.4\%$ and $\epsilon^p = 5\%$. An important point is the appearance of the second order behaviour both in the experiments and simulations, illustrated by the superposition of the curves at 60 and 80 MPa for $\epsilon^p = 0.4\%$. This phenomenon disappears when $\epsilon^p = 5\%$ because the kinematic hardening reaches to push the second-order effect beyond the maximum stress of 80 MPa. One can note a clear difference between the calculated and measured values. This difference is specific to the use of the multi-scale model, as already noted by Daniel et al. [19]. A possible improvement is the inclusion of local demagnetizing fields. Nevertheless, general trends are reproduced, making it possible to identify hardenings. Indeed, knowing the value of c, the measurement of χ_p^0 at 0 MPa allows to determine $R+J_2(\mathbf{X})$. Measuring the initial susceptibility of the plastified sample under different tensile elastic loadings is then used to estimate the value of $J_2(\mathbf{X})$ as in Fig. 3.

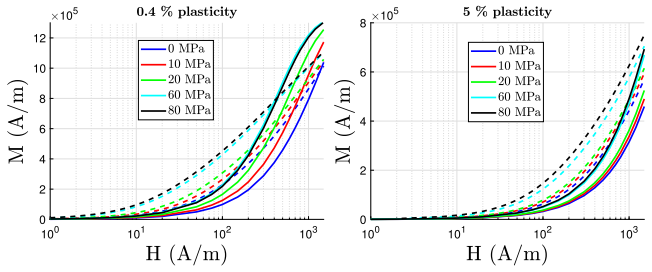

Fig. 4. Simulations (full lines) and measurements (dashed lines) of the magnetization for different stress levels. Left: $\chi_p^0 = 2890$ identified on measurements at $\epsilon^p = 0.4\%$. Right: $\chi_p^0 = 596$ identified on measurements at $\epsilon^p = 5\%$.

5. Conclusion

A full thermodynamic description is proposed to describe both magneto-elastic and magneto-plastic coupling. Eight magneto-elastic coupling constants are used: two first-order and six second-order. The effect of plasticity is taking into account by introducing only one new parameter.

A common limit of this type of study is the difficulty of distinguishing kinematic hardening from isotropic hardening. In order to overcome this, plastification tests will be carried out on electrical steel sheets in compression. Several extensions to this work are also possible. The first is to measure magnetostriction on plastified specimens. The second is to test the model on more complex loads, whether elastic or plastic. Finally, this work opens up the possibility of non-destructive measurement of hardening by magnetic measurement.

CRediT authorship contribution statement

J. Taurines: Writing – review & editing, Writing – original draft, Validation, Software, Methodology, Investigation, Conceptualization. **F. Martin:** Methodology, Investigation, Conceptualization. **P. Rasilo:** Supervision, Resources, Funding acquisition, Conceptualization. **A. Belahcen:** Supervision, Resources, Funding acquisition, Conceptualization.

Declaration of competing interest

The authors declare the following financial interests/personal relationships which may be considered as potential competing interests: Anouar Belahcen reports financial support was provided by Research Council of Finland (previously Academy of Finland).

Data availability

No data was used for the research described in the article.

Acknowledgements

This work was supported by the Research Council of Finland under grant number 346438, Centre of Excellence in High-Speed Electromechanical Energy Conversion Systems.

References

[1] R.M. Bozorth, H.J. Williams, Effect of small stresses on magnetic properties, Rev. Modern Phys. 17 (1) (1945) 72.
[2] W.P. Mason, A phenomenological derivation of the first- and second-order magnetostriction and morphic effects for a Nickel crystal, Phys. Rev. 82 (5) (1951) 715–723.
[3] A. Qureshi, L. Chaudhary, Influence of plastic deformation on coercive field and initial susceptibility of Fe-3.25% Si alloys, J. Appl. Phys. 41 (3) (1970) 1042–1043.
[4] J. Makar, B. Tanner, The in situ measurement of the effect of plastic deformation on the magnetic properties of steel: Part I – Hysteresis loops and magnetostriction, J. Magn. Magn. Mater. 184 (2) (1998) 193–208.
[5] P. Shi, et al., The magneto-elastoplastic coupling effect on the magnetic flux leakage signal, J. Magn. Magn. Mater. 504 (2020) 166669.
[6] M. Domenjoud, L. Daniel, Effects of plastic strain and reloading stress on the magneto-mechanical behavior of electrical steels: Experiments and modeling, Mech. Mater. 176 (2023) 104510.
[7] O. Hubert, S. Lazreg, Two phase modeling of the influence of plastic strain on the magnetic and magnetostrictive behaviors of ferromagnetic materials, J. Magn. Magn. Mater. 424 (2017) 421–442.
[8] J. Taurines, et al., Modeling of the morphic effect using a vanishing 2nd order magneto-elastic energy, J. Magn. Magn. Mater. 570 (2023) 170471.
[9] E. du Trémolet de Lacheisserie, Magnetoelastic properties of amorphous alloys, J. Magn. Magn. Mater. 25 (3) (1982) 251–270.
[10] J. Lemaitre, et al., Mécanique des Matériaux Solides, Dunod, 2009.
[11] L. Daniel, et al., Reversible magneto-elastic behavior: a multiscale approach, J. Mech. Phys. Solids 56 (3) (2008).
[12] S. Chikazumi, Physics of Ferromagnetism, Oxford University Press, 1997.
[13] N. Buiron, et al., A multiscale model for magneto-elastic couplings, J. Phys. IV Fr. 9 (PR9) (1999) Pr9–187.
[14] O. Hubert, Multiscale magneto-elastic modeling of magnetic materials including isotropic second order stress effect, J. Magn. Magn. Mater. 491 (2019) 165564.
[15] A. Seeger, et al., Effect of lattice defects on the magnetization curve of ferromagnets, J. Appl. Phys. 35 (3) (1964) 740–748.
[16] Z. Maazaz, et al., Influence of plastic compression on the magnetic behaviour of a pipeline steel, in: SMM25, 2022.
[17] M. Sablik, et al., Modeling of sharp change in magnetic hysteresis behavior of electrical steel at small plastic deformation, J. Appl. Phys. 97 (10) (2005) 10E518.
[18] N. M'zali, et al., Finite-element modeling of magnetic properties degradation due to plastic deformation, IEEE Trans. Magn. 56 (2) (2020) 1–4.
[19] L. Daniel, M. Rekik, O. Hubert, A multiscale model for magneto-elastic behaviour including hysteresis effects, Arch. Appl. Mech. 84 (9–11) (2014) 1307–1323.